Axis projection for Kidney-Region-Of-Interest detection in computed tomography

Tomasz Les
Warsaw University of Technology
Warsaw, Poland
lest@ee.pw.edu.pl

Tomasz Markiewcz
Warsaw University of Technology
Military Institute of Medicine
Warsaw, Ponad
markiewt@iem.pw.edu.pl

Miroslaw Dziekiewicz
Military Institute of Medicine
Warsaw, Poland
dziekiewicz@wp.pl

Malgorzata Lorent
Military Institute of Medicine
Warsaw, Poland
mlorent@wim.mil.pl

***Abstract*— The article presents an innovative method of scanning slices in computed tomography. The presented technique allows for automatically generation of three-dimensional projection, determined by X-Y-Z surfaces. Projections allow to calculate Kidney-Region-Of-Interest - a minimal envelope of kidney contours for all CT scans. The presented technique increases the accuracy of automatic identification and segmentation of kidneys and can be a good starting point for other techniques for identifying kidney areas on individual CT scans. This method significantly limits the area of kidney searching, thereby accelerates the operation of identification for any algorithm. The presented method is based on the technique of pixel intensity values averaging, area region-growing algorithms and morphological transformations. The presented technique has also been tested in implementation of the U-Net neural network system. Our presented solution of X-Y-Z projection is characterized by a high efficiency of visualization, comparable to the results obtained by a human expert.**

Keywords—kidney, projection, region-growth, U-Net, detection

I. INTRODUCTION

The development of computer-aided techniques for supporting medical diagnostics allows obtaining better treatment effects, increasing the accuracy of a disease diagnosis as well as increasing the survival rate of ill people. The development of image processing techniques in imaging diagnostics, such as computed tomography, x-ray or ultrasound, is especially important. This work presents the technique of computerized tomography (CT) image processing technique, which allows obtaining precise areas limiting the occurrence of the kidney in three dimensions X-Y-Z. Medical-imaging of kidneys is used as the basic stage in the diagnosis and treatment of cancer. Kidney cancer occurrence is on the sixth place among men and eighth among women [1, 2]. The development of new methods for visualization of medical data, as well as automatic image processing methods for kidney detection is a very valuable tool for pathologist, oncologist, and other medical specialists [3].

Currently, many automatic kidney detection techniques in CT images have been published. A lot of presented techniques are based on area segmentation methods, such as K-means, watershed and region-growing algorithms [4, 5, 6, 14]. These types of techniques are characterized of kidney-boundary recognition at level of 86%, which is close to a human expert. The second group of techniques widely described in the literature and used in practice worldwide are methods based on machine learning. Algorithms based on neural networks such as U-Net are very often used. These systems have the efficiency in recognizing kidney contours at level of 90% [7, 8]. The disadvantages of this type of solutions are slow data analysis time, high hardware requirements and a long learning time process. Other solutions basing on hybrid methods are often used, combining learning techniques and morphological techniques for image processing [9].

Regardless of the method of data analysis, the presented systems have a common feature - they analyze each CT slice separately. The number of scans to be analyzed for one patient is from several to several hundred - depending on the density of the tomographic scanner properties. This means that the algorithm that performs image segmentation must process the entire field of view several hundred, even up to 300 times - for CT images with a size of 512x512 pixels = 262144 pixels. The technique we developed allows for significant limitation of the kidney search area to a certain subset area that covers the minimum possible area in which all kidney contours are included. This area usually does not exceed 10,000 pixels, which is 3.81% of the potential search area. In addition, the innovative projection technique presented in this article allows the visualization of scans in three X-Y-Z dimensions, which further increases the possibilities of analyzing data from a completely new perspective.

II. PROBLEM STATEMENT

Single computed tomography examination allows to obtain *H* scans in the form of digital gray-scale images. Expectations towards computer systems supporting medical diagnostics in computed tomography are focused mainly on the possibility of an automatic identification of the borders of selected organs, e.g. kidneys. In this article, we do not present a complete method to identify the exact border of the kidney in each separate slice. The technique we propose allows for universal finding of a minimal subset of data that certainly contains the entire kidney border -

This work has been supported by the National Science Centre (2016/23/B/ST6/00621 grant), Poland.

978-1-7281-6926-2/20/$31.00 ©2020 IEEE

Kidney-Region-Of-Interest (KROI) and visualization of this set in three X-Y-Z dimensions. This limited subset can be further analyzed by any other segmentation algorithm.

The following designations have been introduced: projection X, projection Y and projection Z, divided into Z1 and Z2. Each projection visualizes data in a different dimension. All three projections are presented in Fig. 1.

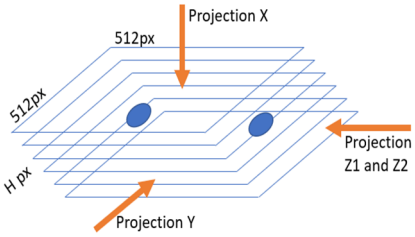

Fig 1. Visualization of the X projection, Y projection and Z1 and Z2 projections. The blue area represents the position of the kidneys.

Projection X is the most used projection in the CT images analysis. It represents the body's projection from the head down. This projection is also most used in image processing algorithms for automatically kidneys detection. Works: [4-9] use the X projection as the main visualization mode. An example of CT image in the X projection is shown in Fig. 2.

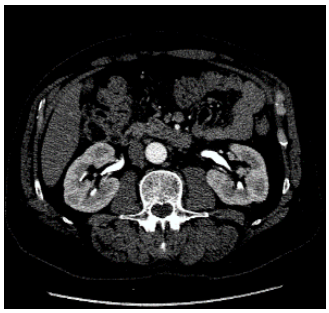

Fig 2. An example of CT image showing the abdominal segment, with visible kidneys.

Projection X is most often used in image segmentation algorithms because it is easy to determine the first and the last slice containing the kidney. Other organs such as liver, spleen and spinal cord are also visible in this projection. The projection Y presents the body from the abdomen to the back, which is much more demanding in analysis. It is much more difficult to determine the first and last slice, containing the kidney, because the location of the kidney can vary significantly in many patients. In addition, each patient has a different fat thickness, which also affects the location of the kidney. Similar problems occur in the Z projection. In this case, there is another problem related to the fact that in this projection two kidneys overlap. To circumvent this problem, the Z projection was divided into Z1 and Z2 projection, generating visualization for the left and right kidneys, respectively. The challenge in Y, Z1 and Z2 projection is to find the first and the end slice so that other organs do not cover the kidney. In fig. 3 the lines limiting the projection Y and the projection Z2 for the enlarged kidney from fig 2 are shown.

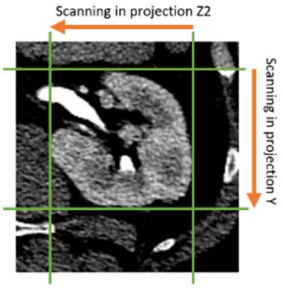

Fig 3. Kidney boundaries in projection Y and Z2.

The following chapters present the projection technique of Y, Z1 and Z2, together with the algorithm of finding the KROI area in this projection.

III. Methods of CT scans projection

This chapter describes how to create X-Y-Z projections for all scans of a given patient. In the first step, we prepare a set of scans $s_1 \ldots s_n$ in the basic projection X. The first scan - s_1 and the end scan s_n are the first and the last scans containing the kidney. In the next step, projection X - $projX$ is created. We generate a new image where each pixel is the average of all pixels of all slices with the same coordinates according to formula (1):

$$projX(x,y) = \frac{s_1(x,y) + \cdots + s_n(x,y)}{n} \qquad (1)$$

The result of the performed operation is presented in Fig. 4.

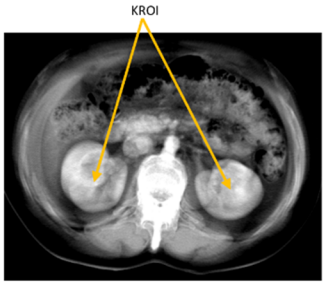

Fig 4. Projection X, which is an average of all slices from 1 ... n and the KROI area indicated.

The new image shows KROI areas, forming the field of kidney search for each of the slices $1..n$.
Projections Y, Z1 and Z2 are generated in a similar way. In this case, we sum pixels in the Y or Z axis, but only in the area bounded by the green lines (fig. 3). The result of the projection Y, Z1 and Z2 is shown in figure 5.

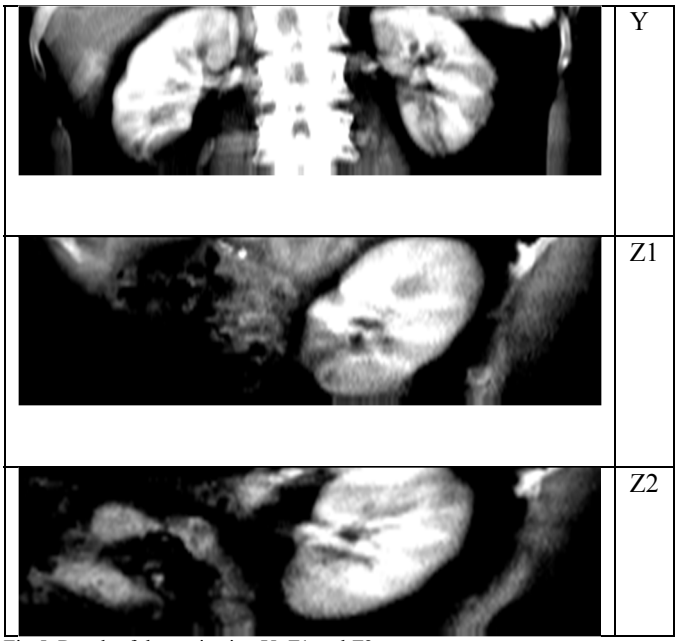

Fig 5. Result of the projection Y, Z1 and Z2.

Projection Y contains two KROI areas. Projections Z1 and Z2 contain only one KROI area. It is mandatory to precisely define the first and last slice ($s_1 \dots s_n$) for generation process of Y, Z1 and Z2 projections. This is possible after using the KROI detection algorithm for projection X. Slices $s_1 \dots s_n$ for projection Y are determined by the points $x_{1\dots512}, y_{min}$ and $x_{1\dots512}, y_{max}$. Slices $s_1 \dots s_n$ for the projection Z are determined by the points $x_{min}, y_{1\dots512}$ and $x_{max}, y_{1\dots512}$, separately for the left and right kidneys. In the following sections, techniques for KROI calculation for each projection are presented.

A. Fully automated KROI detection system

This chapter introduces two techniques for automatic KROI detection: region-growth based technique and U-Net assisted segmentation. These techniques can be used independently or combined.

B. Region-growth segmentation

The region-growth segmentation technique is based on the region-growing algorithm. The algorithm is performed on each image separately. We analyze images representing results of projection X, Y, Z1, Z2. First step in this algorithm is to set initial points for region-growth.
We have calculated two square areas: A and B according to following rules:

- Area A: {X1: 125, Y1:250}, {X2: 225, Y2:350},
- Area B: {X1: 287, Y1:250}, {X2: 387, Y2:350},

Figure 6 shows the marked areas.

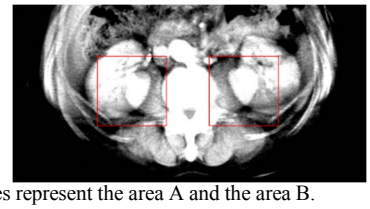
Fig 6. Red squares represent the area A and the area B.

Region-growth is performed at every point inside the area A and the area B, with a step of x and y = 25px. In total 25 region-growths are made. The growth-stop criterion is the growth-area cannot exceed the value of 50000px. For each generated area we calculate geometric coefficient of circularity - cf and we finally select the area with the largest value of cf.

$$cf = \frac{4\,\pi\,S}{C} \tag{2}$$

According to above formula S is a surface area and C is a circuit of binary result of region-growth. Finally, a morphological dilate operation, with 4px size structural element, is performed. This operation is performed to ensure that the found KROI area will cover all potential kidney boundaries for each CT slice.

C. U-Net assisted segmentation

In this section we present another segmentation technique, based on machine learning using the U-Net. U-Net is a multi-layer neural network. The input layer of the network are the dimensions of the data [12,13]. In network learning process, the following parameters have been set to following:

- no of epoch: 20,
- learning algorithm: sgdm,
- minimum batch size: 256,
- gradient threshold: 0.05,
- the initial learning rate: 0.05,
- the L2 regularization: 0.0002,
- the momentum: 0.95.

Image data for network learning process are CT scans for 96 cases. In total, 4534 CT slices were analyzed. The network was then tested on another set of 1303 CT slices as testing data. The predicted network result is a set of gray-scale images. Each pixel intensity value corresponds to the number of votes cast by the network that this point is a part of the kidney area. Then, projections X-Y-Z were made for each case, according to the technique presented in the previous chapter. Both the region-growth technique and the technique based on the neural network allow for each case to obtain a precise area -KROI, in which all kidney borders for each CT slice are included. Fig 7 shows the result of the projection X, as well as the result of region-growth algorithm (the red outline) and the U-Net result (the area found is visible in the form of gray-scale). The results obtained for two cases: A and B were also compared to the sum of human expert masks calculated for each CT slice in the X projection.

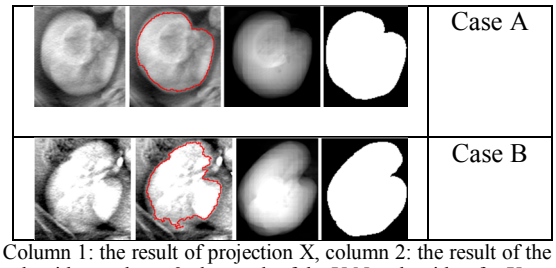

Fig 7. Column 1: the result of projection X, column 2: the result of the region-growth algorithm, column 3: the result of the U-Net algorithm for X projection, column 4: a reference to the mask of a human expert.

Similar results can be obtained for other projections: Y, Z1 and Z2. The image results are shown in Fig. 8.

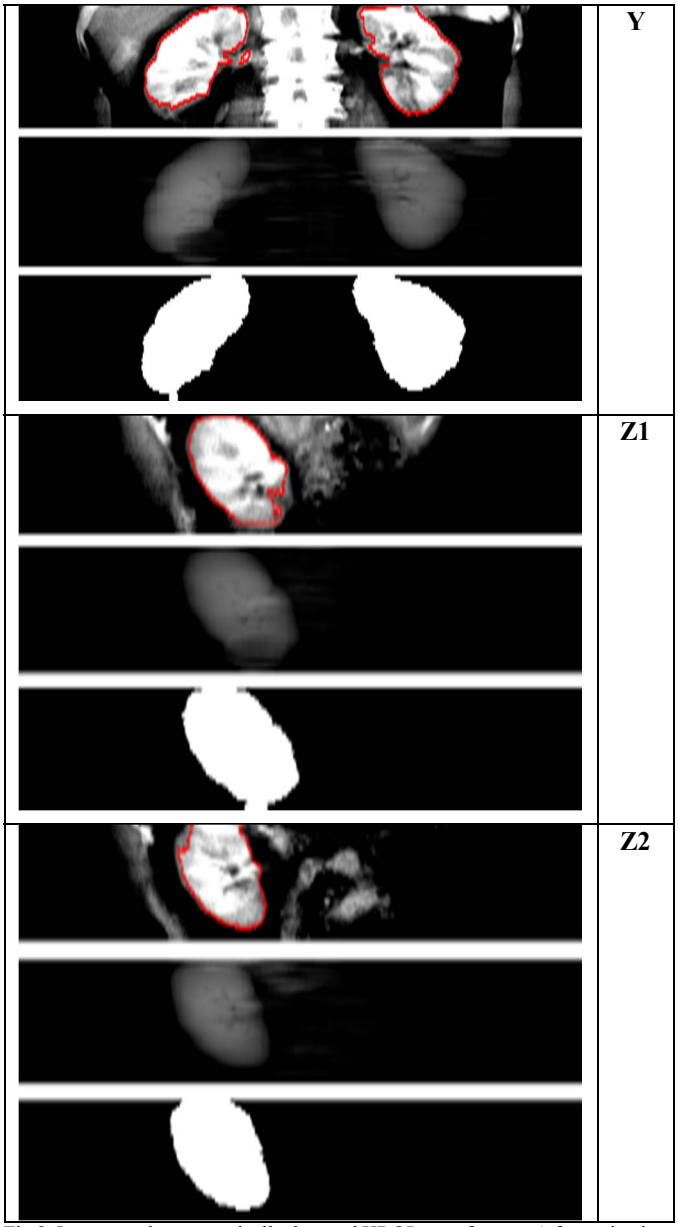

Fig 8. Image result: automatically detected KROI areas for case A for projections Y, Z1 and Z2.

The same experiment was performed for case B. The results of the KROI detection are visible on Fig. 9. For each projection, top image represents region-growth algorithm effect, middle image represents U-Net result and bottom image represents expert mask.

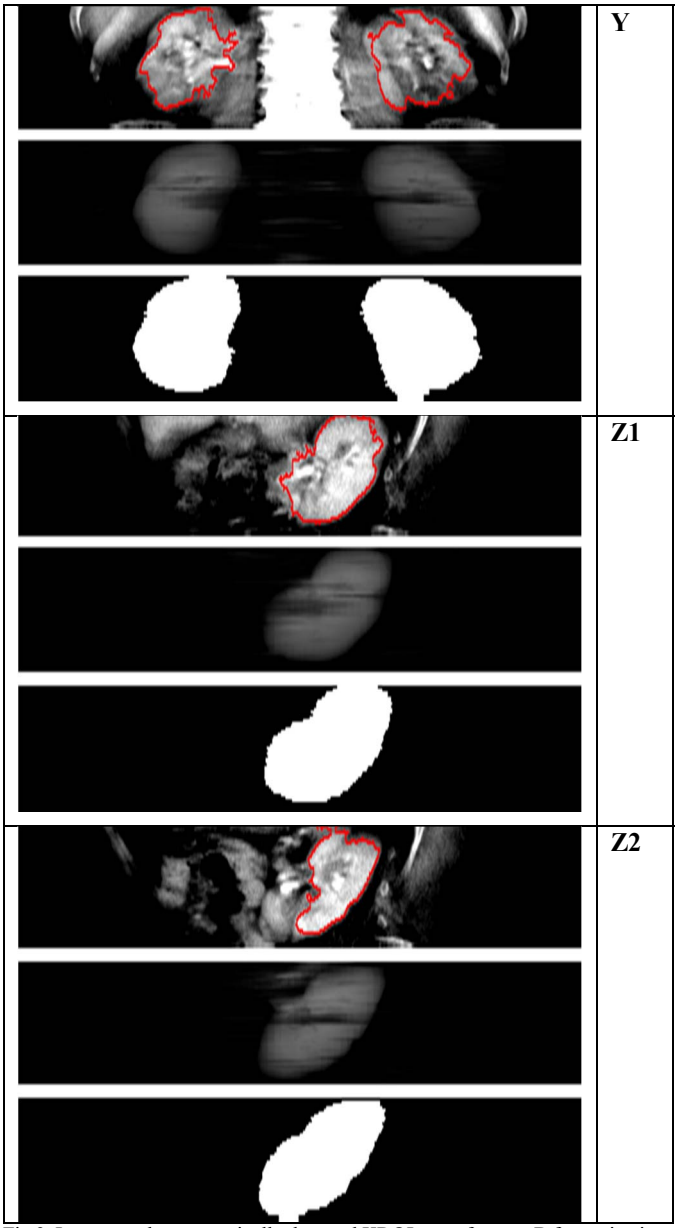

Fig 9. Image result: automatically detected KROI areas for case B for projections Y, Z1 and Z2.

The graphic presentation of the results allows to notice a high compatibility of the automatically detected KROI areas with the area marked by the expert in each of the X-Y-Z projections, both for the region-growth algorithm and the algorithm based on the U-Net network. In order to compare the obtained results, numerical tests were performed, presented in the next section. A full diagram showing the main steps of the complete KROI

detection system, using a region-growth technique is shown in Figure 10.

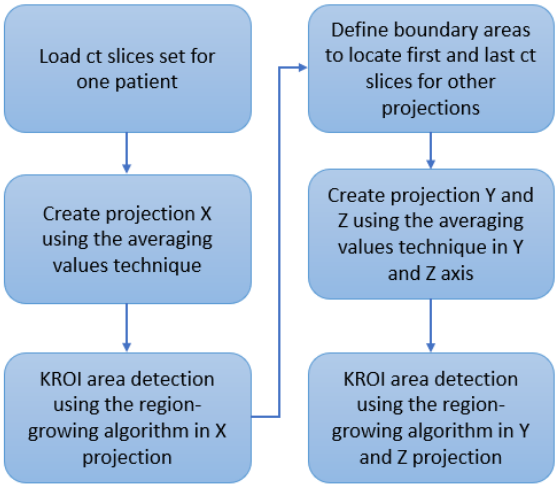

Fig 10. A full diagram showing the main steps of the complete KROI detection system, using a region-growth technique.

Figure 11 presents another diagram showing the main steps of the KROI detection system using a method based on the U-Net network model.

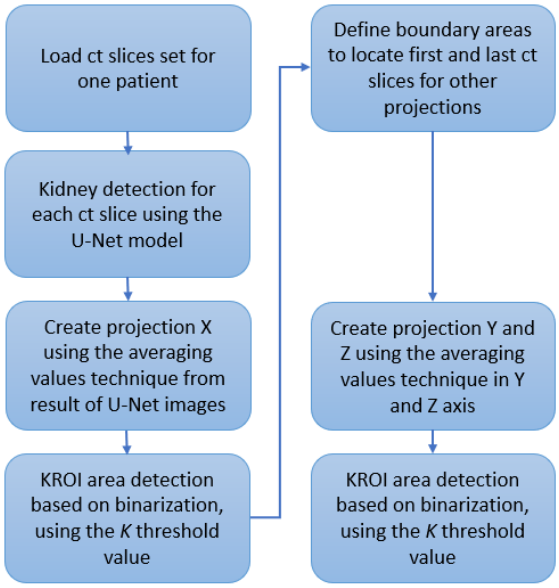

Fig 11. A full diagram showing the main steps of the complete KROI detection system, based on the U-Net network model.

IV. TESTS AND RESULTS

Numerical tests have been developed to assess the possibilities of the presented algorithms. We tested 26 cases. Each case is made up of average 50 CT slices. In total, 1303 CT slices were analyzed. The tested images come from the archives of the Military Institute of Medicine in Warsaw, Poland. The images in raw format were analyzed using the MATLAB environment [11] by an algorithm based on region-growth and the technique using the U-Net. The result of the region-growth algorithm is in the form of a binary mask. The U-Net result is a gray-scale image. In order to compare both solutions, for U-Net result images we applied threshold of value $k = 32$, to obtain a binary image. In order to select the optimal value of k, we applied a ROC cure (receiver operating characteristic curve) analysis. The ROC analysis allows to determine the dependence of sensitivity and specificity. Figure 12 shows the ROC chart. On the horizontal axis, the threshold values K was determined. The analysis of many cases allowed the selection of the optimal threshold value (K).

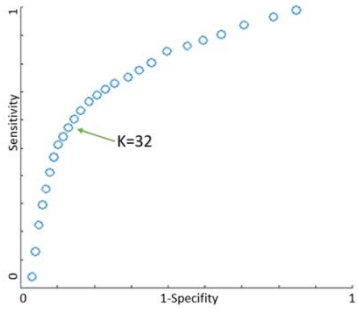

Fig 12. ROC cure analysis allows the selection of the optimal K value in order to binarize the U-Net image result.

Both binary images (result of region-growth and U-Net) were compared to the masks of an expert from the Military Institute of Medicine, who manually marked all scans. The numerical results represent the Sørensen-Dice measure [10], commonly used to evaluate the effectiveness of KROI detection algorithms. Each projection X-Y-Z was tested independently. Table I presents numerical results of KROI detection accuracy for X-Y-Z projections for region-growth algorithm.

TABLE I. NUMERICAL RESULTS OF THE KROI DETECTION ACCURACY FOR X-Y-Z PROJECTION FOR REGION-GROWTH ALGORITHM.

Group	Total CT slices in group	KROI accuracy in projection			
		X	Y	Z1	Z2
1	104	66.74	74.93	90.06	82.64
2	97	84.22	93.67	78.11	91.88
3	90	80.58	91.07	73.82	96.96
4	103	97.71	79.31	86.39	79.45
5	91	79.41	72.97	74.47	96.26
6	86	88.17	97.26	78.02	74.07
7	107	74.77	72.66	75.25	83.58
8	143	75.88	72.34	87.54	91.33
9	87	85.58	87.63	81.79	84.13
10	47	90.76	82.96	97.23	92.97
11	95	82.97	83.29	89.23	95.62
12	138	65.03	83.19	80.39	85.66
13	115	79.81	89.72	93.12	91.19
	Avg:	80.89	83.15	83.49	88.13

The same tests were performed for the segmentation technique based on U-Net.
Table II presents numerical results of KROI detection accuracy for X-Y-Z projections U-Net algorithm.

TABLE II. NUMERICAL RESULTS OF THE KROI DETECTION ACCURACY FOR X-Y-Z PROJECTION FOR U-NET TECHNIQUE.

Group	Total CT slices in group	KROI accuracy in projection			
		X	Y	Z1	Z2
1	104	75.34	93.34	98.86	76.13
2	97	88.32	78.56	81.41	98.77
3	90	88.08	86.34	77.02	94.57
4	103	98.96	93.13	94.19	79.31
5	91	86.17	87.46	84.97	74.97
6	86	80.43	93.24	86.12	90.76
7	107	84.91	91.58	84.75	80.78
8	143	81.58	98.33	90.24	94.01
9	87	81.58	94.73	89.29	86.25
10	47	99.14	99.37	81.02	97.86
11	95	78.71	92.78	96.23	72.25
12	138	90.97	91.16	87.09	91.87
13	115	95.27	99.49	84.13	91.22
	Avg:	86.88	92.27	87.33	86.83

Analysis of Tables I and II shows that for projections X, Y and Z1, the recognition of KROI is more accurate for U-Net technique. In projection Z2 the KROI region is better recognized, for the technique of region-growth. In tables I and II, the unique cases are divided into 14 groups. For each group the total number of CT slices and average KROI detection accuracy was given. Each group contains images of two randomly selected patients. The total number of patients whose cases we analyzed is 26.

The developed numerical results show that the average accuracy of KROI recognition for region-growth is 80%-88%, while for the algorithm based on the U-Net network it is 86%-92%.

V. CONCLUSION

The article presents an innovative CT slices projection method in projection X-Y-Z. Our visualization allows for defining the KROI area - kidney region of interest, which includes all the borders of the kidneys. Two different approaches have been tested for KROI detection: technique based on region-growth processing, and machine learning approach - U-Net. Both solutions were compared to human expert binary masks. The main features of the presented solutions are the following:

- Region-growth: fast operation time, no requirement of a large data learning set, no high hardware requirements.
- U-Net: the need to analyze large data sets, high hardware requirements, the need for post-processing to get the final binary mask.

The benefits of using the developed techniques are:

- Shortening the calculation time for any kidney identification algorithm (since the search area is significantly limited),
- Increasing the accuracy of any kidney identification algorithm (by omitting areas incorrectly detected - false-positive error)
- The ability to visualize the projection in different projections: X-Y-Z (which allows the use of new, alternative data segmentation methods)

We performed numerical tests that confirmed the high efficiency of KROI identification of both presented methods. The evaluated techniques can be used alternatively and are good starting point for any algorithm for kidney localization in individual CT slice.

The development of new methods of analysis and processing of image data is necessary in order to increase the possibilities of medical diagnostics. It is necessary to further develop the methods and new algorithms, including hybridization of different solutions.

REFERENCES

[1] http://www-dep.iarc.fr/WHOdb/WHOdb.htm

[2] H. Moch, P. A. Humphrey, T. M. Ulbright, V. E. Reuter, editors, "WHO Classification of Tumours of the Urinary System and Male Genital Organs" (4th edition), IARC, Lyon, 2016.

[3] J. Ferlay, M. Ervik, F. Lam, M. Colombet, L. Mery, M. Pineros, A. Znaor, I. Soerjomataram, F. Bray, Global Cancer Observatory: Cancer Today. Lyon, France: International Agency for Research on Cancer. 2018. Available from: https://gco.iarc.fr/today, accessed [25 November 2019].

[4] M. Mohammad, Z. Kraitem, "Automatic Detection and Segmentation of Kidneys in Magnetic Resonance Images Using Image Processing Techniques", Biomedical Statistics and Informatics 2 (2017) 22-26.

[5] D. Lin, L. Chung-Chih, H. Siu-Wan, "Computer-Aided Kidney Segmentation on Abdominal CT Images", IEEE Transactions on Information Technology in Biomedicine 10 (2006) 59-65.

[6] M. Myint, T. Myint, "Effective Kidney Segmentation Using Gradient Based Approach in Abdominal CT Images", in: Proceedings of 2015 International Conference on Future Computational Technologies (ICFCT'2015) Singapore, March 29-30, 2015, pp. 130-135.

[7] D.C. Cireşan, A. Giusti, L.M. Gambardella, J. Schmidhuber, "Mitosis Detection in Breast Cancer Histology Images with Deep Neural Networks", in: Medical Image Computing and Computer-Assisted Intervention – MICCAI 2013. Springer, Lecture Notes in Computer Science 8150 (2013) 411-418.

[8] M. Karabatak, M. Cevdet Ince, "An expert system for detection of breast cancer based on association rules and neural network", Expert Systems with Applications 36 (2009) 3465-3469.

[9] T. Les, T. Markiewicz, S. Osowski, W. Kozlowski, M. Jesiotr, "Fusion of FISH image analysis methods of HER2 status determination in breast cancer", Expert Systems with Applications, 2016

[10] N. Heller, N. Sathianathen, A. Kalapara, The KiTS19 Challenge Data: 300 Kidney Tumor Cases with Clinical Context, CT Semantic Segmentations, and Surgical Out-comes"

[11] https://www.mathworks.com

[12] Y. LeCun and Y. Bengio, "Convolutional networks for images, speech, and time series", The handbook of brain theory and neural networks 3361 (10), 1995

[13] Y. LeCun, L. Bottou, Y. Bengio, P. Haffner, "Gradient-based learning applied to document recognition". In Proceedings of the IEEE 1998, 86:2278-2324.

[14] T. Les, T. Markiewicz, M. Dziekiewicz, M. Lorent, "A Flood-Fill-Based Technique for Boundary Closure of Kidney Contours in CT Images", International Conference on Global Research and Education, 2018, pp. 225-232